Matrix Isolation and Density Functional Study of the Reaction of $OVCl_3$ with CH_3SH

Bruce S. Ault

Department of Chemistry, University of Cincinnati, P.O. Box 210172, Cincinnati, Ohio 45221-0172

Received: July 26, 2000; In Final Form: October 17, 2000

The matrix isolation technique has been combined with infrared spectroscopy to isolate, identify, and characterize the initial intermediates in the thermal and photochemical reactions of $OVCl_3$ with CH_3SH. The thermal reaction proceeds through formation of a 1:1 complex that is characterized by perturbations to the $-VCl_3$, $-V{=}O$, and S−H stretching modes, as well as the $-CH_3$ rocking and bending modes. The photochemical reaction leads to HCl elimination from the initial 1:1 complex, and formation of $Cl_2V(O)$-SCH_3. Additional support for the species identification and vibrational band assignments comes from isotopic substitution. Density functional calculations (B3LYP/6-311G+(d, 2p)) were carried out to confirm the experimental band assignments for this latter species. Efforts to study the thermal reaction beyond formation of the initial complex were unsuccessful, despite pyrolysis at temperatures as high as 300 °C prior to sample deposition.

Introduction

High valent transition metal oxo compounds, including $OVCl_3$, are often used as potent yet selective oxidizing agents in organic synthesis.[1,2] However, little is known about the details of the reaction mechanism, and the features that lead to selective oxidation. On the other hand, a number of theoretical calculations on such systems have been carried out in recent years, with the intent of providing a better understanding of the pathways, intermediates, and energetics for these reactions.[3−7]

The matrix isolation technique[8−10] was developed to facilitate the isolation and characterization of reactive intermediates. This approach has been applied to the study of a wide range of species, including radicals, ions, and weakly bound molecular complexes. A recent matrix isolation study examined the reaction between $OVCl_3$ and CH_3OH, and identified three different steps in the reaction mechanism.[11] Different deposition conditions were used to observe sequential intermediates in the reaction pathway. The degree to which the analogous sulfur compound, CH_3SH, will follow the same pathway is not known, and resolution of this question may provide insights into process of selective oxidation of organic substrates. Consequently, a study was undertaken to examine the reaction of $OVCl_3$ with CH_3SH, followed by trapping in argon matrices. Density functional calculations were also carried out in support of the experimental observations.

Experimental Section

All of the experiments in this study were carried out on conventional matrix isolation apparatus that has been described.[12] Oxyvanadium trichloride, $OVCl_3$ (Aldrich), was introduced into the vacuum system as the vapor above the room-temperature liquid, after purification by freeze−pump−thaw cycles at 77 K. CH_3SH (Aldrich) and CH_3SD (CDN Isotopes, >91% D) were introduced from lecture bottles into separate vacuum manifolds and were purified by repeated freeze−pump−thaw cycles at 77 K. Argon was used as the matrix gas in all experiments and was used without further purification.

Matrix samples were deposited in both the twin jet and merged jet modes. In the former, the two gas samples were deposited from separate nozzles onto the 14 K cold window, allowing for only a very brief mixing time prior to matrix deposition. A number of these matrices were subsequently warmed to 33−35 K to permit limited diffusion and then recooled to 14 K and additional spectra recorded. In the merged jet mode,[13] the two deposition lines were joined with an Ultratorr tee at a distance from the cryogenic surface, and the flowing gas samples were permitted to mix and react during passage through the merged region. The length of this region was variable; typically, a 50 cm length was employed. In addition, the merged region could be heated to as high as 300 °C to induce further reaction. Some matrices were deposited using slow deposition, with a flow rate of 1 mmol/h from each manifold for 20−24 h before the recording of final spectra. Other matrices were deposited in a rapid mode, with flow rates of 6 mmol/h from each line, typically for 3 h of deposition. In either case, final spectra were recorded on a Nicolet IR 42 Fourier transform infrared spectrometer at 1 cm^{-1} resolution.

Theoretical calculations were carried out on likely intermediates in this study, using the Gaussian 94 suite of programs.[14] Density functional calculations using the Becke B3LYP functional were used to locate energy minima, determine structures, and calculate vibrational spectra. Final calculations with full geometry optimization employed the 6-311G+(d,2p) basis set, after initial calculations with smaller basis sets were run to approximately locate energy minima. Calculations were carried out on a Silicon Graphics Indigo 2 workstation.

Results

Prior to conducting any co-deposition experiments, blank experiments were carried out on each of the reagents in this study. The resulting spectra were in good agreement with literature spectra, and with spectra previously recorded in this laboratory.[15,16] These blank spectra were also irradiated with the H_2O/Pyrex-filtered output of a 200 W Hg arc lamp, and additional spectra recorded. No changes were observed as a result of irradiation.

In an initial merged jet experiment, a sample of $Ar/CH_3SH = 250$ was co-deposited with a sample of $Ar/OVCl_3 = 500$,

10.1021/jp002683a CCC: $19.00
Published on Web 11/16/2000

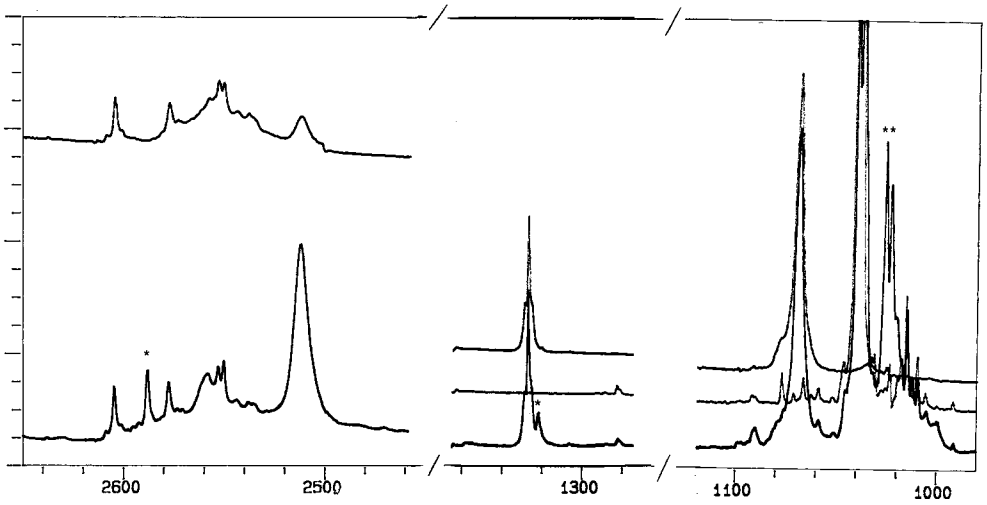

Figure 1. Infrared spectra in several spectral regions of the matrix formed by the merged jet co-deposition of a sample of $Ar/CH_3SH = 100$ with a sample of $Ar/OVCl_3 = 500$, compared to a blank spectrum of a sample of $Ar/CH_3SH = 100$ (upper trace in the left-hand portion of the plot; top trace in the center and right-hand portions of the figure) and a blank spectrum of a sample of $Ar/OVCl_3 = 500$ (middle trace in the center and right-hand portions of the figure). Bands marked with an asterisk (∗) are due to the 1:1 complex.

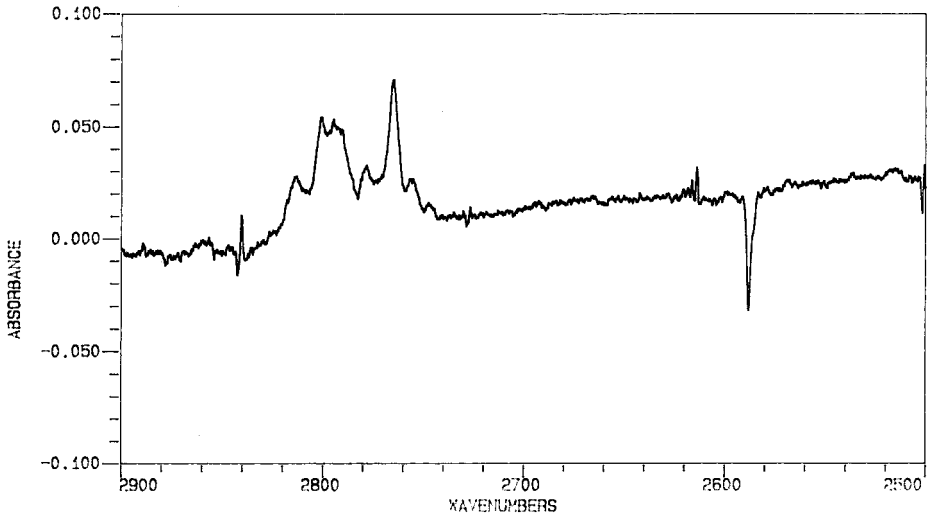

Figure 2. Difference spectrum arising from the spectra taken before and after irradiation of a matrix containing the 1:1 complex between $OVCl_3$ and CH_3SH, in the 2500−2900 cm^{-1} region. Note decrease of the band due to the complex near 2588 cm^{-1} and the growth of a multiplet with its most intense component at 2765 cm^{-1}.

using a room-temperature merged region. Four new weak-to-medium bands were seen in the resulting spectrum, at 430, 1025, 1321, and 2588 cm^{-1}. In several subsequent experiments, the temperature of the merged region or reaction zone was heated to as high as 300 °C. In all these experiments, the same four product bands were observed, and no additional product bands were seen. An initial twin jet experiment was then run using the same sample concentrations, and a virtually identical spectrum was obtained. The four bands listed above were seen, and no additional bands were noted. In as much as the same product bands were observed in both the twin jet and merged jet modes, all subsequent experiments were conducted in the merged jet mode, with a room temperature reaction zone.

A number of additional experiments were conducted in which the concentration of the two reactants were varied, between 500/1 and 100/1. When the concentration of either reactant (or both) was increased, the above four product bands were seen with increased intensity. At the same time, these four bands maintained a constant intensity ratio with respect to one another. In addition, weaker bands were seen near 440, 970, and 1431 cm^{-1}. The intensity of these bands also appeared to vary directly as the concentration of the precursors was changed and thus vary directly with the initial four bands described above. In the most concentrated experiments ($Ar/OVCl_3 = 250$ and $Ar/CH_3SH = 100$), the intensities of these product bands were quite high, approaching 1.0 O.D for the most intense bands (at 430 and 1025 cm^{-1}). Several of these matrices were subsequently annealed to 35 K and then recooled to 14 K and additional spectra recorded. In each of these experiments, all seven of the product bands (hereafter referred to as set A) grew as a consequence of annealing, and all grew at the same rate. Only a slight decrease in the intensity of the parent bands was noted as a result of annealing. Figure 1 shows spectra displaying several of the set A bands.

Following annealing, a number of the matrices were then irradiated with the H_2O/Pyrex-filtered output of a 200 W Hg arc for 1.0−2.0 h. During the irradiation process, the temperature of the cold window was observed to increase by a few degrees, but not nearly to the extent of annealing. After irradiation was complete, additional spectra were recorded. In a typical experiment, the all of the bands of set A were completely destroyed by irradiation while new absorptions appeared at 490, 1315, 1420, and 2935 cm^{-1} as well as a multiplet with its most intense component at 2765 cm^{-1}, as shown in Figures 2 and 3. In

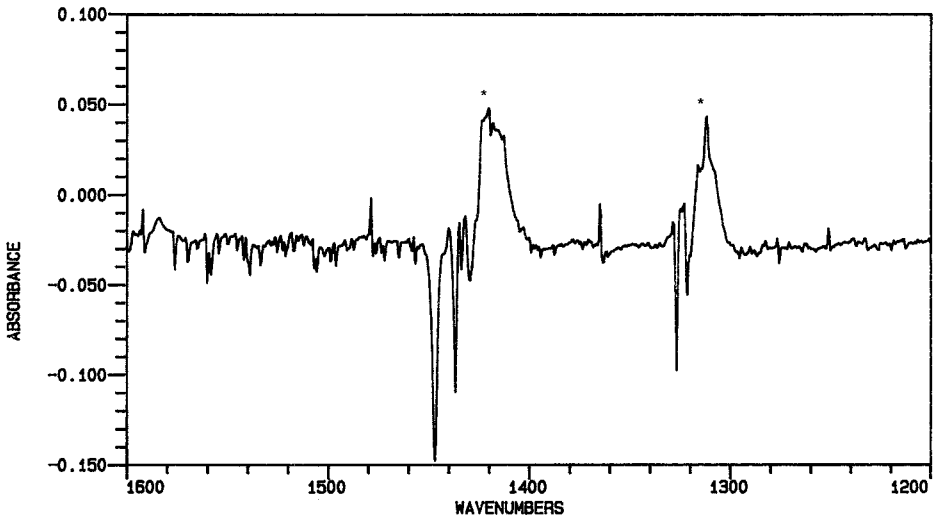

Figure 3. Difference spectrum arising from the spectra taken before and after irradiation of a matrix containing the 1:1 complex between $OVCl_3$ and CH_3SH, in the 1200−1600 cm^{-1} region. Note the decrease of the bands due to the complex near 1321 and 1431 cm^{-1} and the growth of bands at 1315 and 1420 cm^{-1} (marked with an ∗).

TABLE 1: Band Positions (cm^{-1}) and Assignments for the 1:1 Complex of $OVCl_3$ with CH_3SH

$OVCl_3$·CH_3SH	$OVCl_3$·CH_3SD	parent band	assignment
430	430	505	VCl_3 antisym stretch
440	440	505	VCl_3 antisym stretch
970	970	955	CH_3 rock
1025	1025	1040	V═O stretch
1321	1321	1326	CH_3 sym bend
1431	1431	1436	CH_3 antisym bend
2588	1880	2606 (1891)	S−H (S−D) stretch

TABLE 2: Experimental and Computed Band Positions (cm^{-1}) and Assignments for $Cl_2V(O)SCH_3$

expt	computed[a]	assignment
490	491 (476)	VCl_2 antisym stretch
1037	1118 (1084)	V═O stretch
1315	1358 (1317)	CH_3 sym stretch
1420	1476, 1478 (1432, 1434)	CH_3 antisym stretch
2935	3052 (2960)	CH_3 sym stretch

[a] Computed using B3LYP/G-311G+(d,2p). First value listed is unscaled; scaled values (factor of 0.97) given in parentheses.

addition, a new feature was possible at about 1037 cm^{-1}. However, this is within a few wavenumbers of the intense V═O stretching mode of parent $OVCl_3$, and thus identification of a product band in this region is difficult. These bands will hereafter be referred to as set B. These results were reproduced in all of the irradiation experiments, namely complete destruction of the set A bands along with formation of the set B bands. Throughout these experiments, the set B bands maintained a constant intensity ratio with respect to one another.

Experiments were also conducted in which samples of Ar/$OVCl_3$ was co-deposited with samples of Ar/CH_3SD. In an initial merged jet experiment, co-deposition led to the formation of the set A bands in exactly the same locations with the same intensities, with one exception. The 2588 cm^{-1} band observed in set A, above, was no longer present. Instead a weak, distinct band was observed at 1880 cm^{-1}. These bands, too, were reproducible over a range of sample concentrations, maintained a constant intensity ratio with respect one another, and grew distinctly upon annealing the matrices to 35 K. Each of these matrices was subsequently irradiated with the H_2O/Pyrex-filtered Hg arc, and quite similar results were observed. In each of these experiments, bands were again observed at 490, 1037 (tentative), 1315, 1420, and 2935 cm^{-1}. However, the multiplet near 2765 cm^{-1} was now absent, and a new multiplet was observed, with the most intense feature at 2004 cm^{-1}. Table 1 lists all of the set A bands for the reaction of $OVCl_3$ with both CH_3SH and CH_3SD, while Table 2 lists all of the set B bands.

Discussion

Both twin jet and merged jet co-deposition of $OVCl_3$ with CH_3SH into argon matrices at 14 K led to the formation of the set A product bands, at 430, 440, 970, 1025, 1321, 1431, and 2588 cm^{-1}. The observation that these seven bands maintained a constant intensity ratio with respect to one another (to the degree this could be determined for the weaker product bands) in a number of different experiments suggests that they may be assigned to a single product species. This is supported by the fact that they showed the same annealing behavior and the same irradiation behavior. It is also noteworthy that each of these bands was observed relatively near a parent mode of either $OVCl_3$ or CH_3SH; for example, the 2588 cm^{-1} was 18 cm^{-1} to the red of the S−H stretching mode of CH_3SH while the 1025 cm^{-1} band was 15 cm^{-1} to the red of the V═O stretch of $OVCl_3$. Further, the set A bands grew upon annealing to 35 K, indicating that the activation barrier to formation of the product responsible for these bands is very low. At the same time, they were observed during twin jet deposition where the reaction time is very short before formation of the rigid argon matrix. All of these points support identification of the initial product responsible for the set A bands as a molecular complex between $OVCl_3$ and CH_3SH. Molecular complexes, in general, have very low barriers to formation, and result in slight perturbations to the structures and vibrational modes of the two subunits in the complex.

The stoichiometry of the complex is not as readily determined. However, the observation of only a single product after co-deposition over a wide range of concentrations suggests that the stoichiometry is 1:1. Certainly, it would be difficult to envision formation of higher complexes (e.g., 2:1 or 1:2) without also forming the 1:1 complex. The observation of a single product argues against this, and for the formation of the 1:1 complex. Consequently, the set A bands described above are assigned to the 1:1 molecular complex between $OVCl_3$ and CH_3SH. *This species represents the initial intermediate in the reaction between these two compounds.*

Band assignments for the seven observed bands of this complex are straightforward, based on their proximity to parent modes. These assignments are collected in Table 1, for the complexes of $OVCl_3$ with both CH_3SH and CH_3SD. Of note is the band at 2588 cm^{-1}, which is assigned to the perturbed S−H stretch of CH_3SH in the complex. This band shifted to 1880 cm^{-1} upon deuteration while the parent mode shifted from 2606 to 1891 cm^{-1}, strongly supporting this band assignment. Determination of the precise structure of the complex cannot be made from these observations; both the V═O and VCl_3 stretching bands were perturbed in the complex, suggesting that coordination may be at the vanadium center. However, the red shift of the S−H stretching mode suggests that weak hydrogen bonding may be involved as well.

Irradiation of matrices containing the 1:1 complex with light of $\lambda > 300$ nm led to complete destruction of the complex, and the growth of several new infrared absorptions. Of particular note was the multiplet with its strongest component at 2765 cm^{-1}, shown in Figure 2. This multiplet was the only photolysis product band to shift when CH_3SH was replaced by CH_3SD. Specifically, the shift with deuterium substitution was to 2004 cm^{-1}, leading to a ν_H/ν_D ratio of 1.380. The position of this multiplet and its deuterium behavior strongly suggest that this absorption is due to the production of HCl, i.e., that HCl elimination from the complex is occurring. The ν_H/ν_D ratio of 1.38 matches exactly the ratio observed for both gas phase[17] and argon matrix-isolated HCl.[18,19] This result also agrees well the outcome of the irradiation of the $CrCl_2O_2 \cdot CH_3OH$ complex studied earlier, where HCl and $CrClO_2OCH_3$ were formed.[20] However, in that case, and in the present case, the HCl that is formed is not completely isolated by the argon matrix, but rather is cage-paired with the other product(s) of the photolysis. This leads to weak hydrogen bond formation, and a red shift of the H−Cl stretching mode relative to the well-known argon matrix isolated HCl at 2888 cm^{-1}. In the previous study of the $CrCl_2O_2 \cdot CH_3OH$ complex, the H−Cl stretch mode was observed between 2700 and 2800 cm^{-1}, in agreement with the bands observed here. The multiplet structure in both cases probably arises from the multiple hydrogen bonding sites on the second photoproduct.

One or more additional species must be formed as HCl is eliminated from the 1:1 complex. Set B product bands were observed at 490, 1315, 1420, and 2935 cm^{-1}, as well as a possible product band at 1037 cm^{-1}. These bands appeared to be produced with a constant intensity ratio in a number of irradiation experiments, suggesting that they are due to a single absorbing species. The band near 490 cm^{-1} is slightly to the red of the intense antisymmetric VCl_3 stretching mode of parent $OVCl_3$, and is likely due to a V−Cl stretching mode. The bands at 1315 and 1420 cm^{-1} are quite near the $-CH_3$ symmetric and antisymmetric bending modes of parent CH_3SH while the 2935 cm^{-1} is quite near the $-CH_3$ symmetric stretching mode, and are strongly suggestive of the presence of a methyl group in the product. As noted above, the possible product band at 1037 cm^{-1} is very close to the V═O stretching mode of parent $OVCl_3$. Taken together, these observations suggest formation of $Cl_2V(O)SCH_3$, the direct HCl elimination product of the initial molecular complex. This, too, is analogous to the $CrCl_2O_2/CH_3OH$ system where formation of $ClCrO_2OCH_3$ was formed after irradiation. Unfortunately, a number of the vibrational modes of the $-SCH_3$ moiety have quite low infrared intensities and could not be observed.

To further explore possible assignment of the set B bands to $Cl_2V(O)SCH_3$, density functional calculations were undertaken, using the B3LYP functional and the 6-311G+(d, 2p) basis set. These calculations converged to a stable structure for $Cl_2V(O)SCH_3$, indicating that these species is a minimum on the potential energy surface. Calculation of vibrational frequencies for $Cl_2V(O)SCH_3$ indicated that the V−Cl stretches should occur at 491.0 and 491.3 cm^{-1}, and that the V═O stretch of this species should lie 4 cm^{-1} to the red of parent $OVCl_3$. These bands should be the most intense in the spectrum, which matches the experimental observations. The calculations indicate that the next three most intense bands should be the $-CH_3$ symmetric and antisymmetric bending modes and the $-CH_3$ symmetric stretching mode, which were calculated to come at 1358, 1476, 1478, and 3052 cm^{-1}, respectively. These values are unscaled; with a standard scaling factor[21] of 0.97 for B3LYP/6-311, these values scale to 1317, 1432, 1434, and 2960 cm^{-1}, respectively, in good agreement with the 1315, 1420, and 2935 cm^{-1} bands observed experimentally. All of the remaining vibrational bands of $Cl_2V(O)SCH_3$ were calculated to have substantially lower intensities. Thus, the calculated spectrum for $Cl_2V(O)SCH_3$ agrees well with the set B bands here, and lends further support for their assignment. Therefore, the bands at 490, 1315, 1420, and 2935 cm^{-1} as well as the tentative band at 1037 cm^{-1} are assigned to $Cl_2V(O)SCH_3$, observed for the first time in this study. Table 2 lists all of the product bands assigned to $Cl_2V(O)SCH_3$, and compares them to the computed values. Table 3 lists the key structural parameters for $Cl_2V(O)SCH_3$, computed at the B3LYP/6-311G+(d,2p) level.

TABLE 3: Computed[a] Key Structural Features for $Cl_2V(O)SCH_3$

R(V═O)	1.5485 Å	α(Cl−V−O)	111.25°
R(V−Cl)	2.1654 Å	α(Cl−V−Cl)	112.71°
R(V−S)	2.190 Å	α(O−V−S)	100.94°
R(C−S)	1.842 Å	α(H−C−H)	109.61°
R(C−H)	1.087 Å		

[a] Computed using B3LYP/G-311G+(d,2p).

Photochemical reactions of $OVCl_3$ in solution, using either broad band or laser sources, are well-known.[22−24] Thus, it is probable that the $OVCl_3$ subunit in the 1:1 complex provides the electronic transition leading to the absorption of a photon and subsequent elimination of HCl and rearrangement. $Cl_2V(O)SCH_3$, then, is the second intermediate in the photochemical reaction of $OVCl_3$ and CH_3SH. It is interesting that the thermal reaction and rearrangement of the complex did not occur, even at temperatures in the reaction zone as high as 300 °C. Thus, beyond the formation of an initial 1:1 complex, less may be concluded about the mechanism of the thermal reaction of these two compounds. This is in contrast to the recently studied reaction of $OVCl_3$ with CH_3OH, where rapid reaction, with HCl elimination, occurred in merged jet experiments with a room temperature reaction zone. It is likely that the strength of the V−O bond formed in this reaction provides a driving force for rearrangement, while the V−S bond in the present system does not do so. Similar results have been observed[25] in the reaction of CH_3SH with $CrCl_2O_2$.

Acknowledgment. The National Science Foundation is gratefully acknowledged for this support of this work through grant CHE 9877076.

References and Notes

(1) Crans, D. C.; Chen, H.; Felty, R. A. *J. Am. Chem. Soc.* **1992**, *114*, 4543.

(2) Yajima, A.; Matsuzaki, R.; Saeki, Y. *Bull Chem. Soc. Jpn.* **1978**, *51*, 1098.

(3) Deng, L.; Ziegler, T. *Organometallics* **1996**, *15*, 3011.

(4) Deng, L.; Ziegler, T. *Organometallics* **1997**, *16*, 716.
(5) Ziegler, T.; Li, J. *Organometallics* **1995**, *14*, 214.
(6) Rappe, A. K.; Goddard, W. A., III *Nature* **1980**, *285*, 311.
(7) Rappe, A. K.; Goddard, W. A., III *J. Am. Chem. Soc*. **1982**, *104*, 3287.
(8) Craddock, S.; Hinchliffe, A. *Matrix Isolation*; Cambridge University Press: Cambridge, UK, 1975.
(9) Hallam, H. E. *Vibrational Spectroscopy of Trapped Species*; John Wiley: New York, 1973.
(10) Andrews, L., Moskovitz, M., Eds. *Chemistry and Physics of Matrix Isolated Species*; Elsevier Science Publishers: Amsterdam, 1989.
(11) Ault, B. S. *J. Phys. Chem. A* **1999**, *103*, 11474.
(12) Ault, B. S. *J. Am. Chem. Soc*. **1978**, *100*, 2426.
(13) Carpenter, J. D.; Ault, B. S. *J. Phys. Chem.* **1991**, *95*, 3502.
(14) Frisch, M. J.; Trucks, G. W.; Schlegel, H. B.; Gill, P. M. W.; Johnson, B. G.; Robb, M. A.; Cheeseman, J. R.; Keith, T.; Petersson, G. A.; Montgomery, J. A.; Raghavachari, K.; Al-Laham, M. A.; Zakrzewski, V. G.; Ortiz, J. V.; Foresman, J. B.; Cioslowski, J.; Stefanov, B. B.; Nanayakkara, A.; Challacombe, M.; Peng, C. Y.; Ayala, P. Y.; Chen, W.; Wong, M. W.; Andres, J. L.; Replogle, E. S.; Gomperts, R.; Martin, R. L.; Fox, D. J.; Binkley, J. S.; Defrees, D. J.; Baker, J.; Stewart, J. P.; Head-Gordon, M.; Gonzalez, C.; Pople, J. A. *Gaussian 94*, Revision E.1; Gaussian, Inc.: Pittsburgh, PA, 1995.
(15) Filgueira, R. R.; Fournier, L. L.; Varetti, E. L. *Spectrochim. Acta* **1982**, *38A*, 965.
(16) Barnes, A. J.; Hallam, H. E.; Howells, J. D. R. *J. Chem. Soc., Faraday Trans. 2* **1972**, *68*, 737.
(17) Nakamoto, K. *Infrared and Raman Spectra of Inorganic and Coordination Compounds*, 5th ed.; Wiley-Interscience: New York, 1997.
(18) Barnes, A. J.; Hallam, H. E.; Scrimshaw, G. F. *Trans. Faraday Soc*. **1969**, *65*, 3150.
(19) Maillard, D.; Schriver, A.; Perchard, J. P. *J. Chem. Phys*. **1979**, *71*, 505.
(20) Ault, B. S. *J. Am. Chem. Soc*. **1998**, *120*, 6105.
(21) Bytheway, I.; Wong, M. W. *Chem. Phys. Lett*. **1998**, *282*, 219.
(22) Hasenbein, N.; Bandermann, F. *Makromol. Chem*. **1987**, *188*, 83.
(23) Kryukov, A. I.; Trachenko, Z. A.; Kuchmii, S. Ya. *Dokl. Akad. Nauk. SSSR* **1974**, *216*, 592.
(24) Wight, C. A.; Armentrout, P. B. *ACS Symp. Ser*. **1993**, *530*, 61.
(25) Anderson, S. R.; Ault, B. S., unpublished results.